

Theoretical and Electrochemical Studies of Metformin as Corrosion Inhibitor for Mild Steel in Hydrochloric Acid Solution

Ambrish Singh¹, Eno. E. Ebenso², M. A. Quraishi^{1,*}

¹ Department of Applied Chemistry, Institute of Technology, Banaras Hindu University, Varanasi 221 005 (India)

² Department of Chemistry, School of Mathematical and Physical Sciences, North-West University (Mafikeng Campus), Private Bag X2046, Mmabatho, 2735, South Africa

*E-mail: maquraishi.apc@itbhu.ac.in

Received: 19 March 2012 / *Accepted:* 8 April 2012 / *Published:* 1 May 2012

The effect of Metformin was investigated by gravimetric, potentiodynamic polarization and electrochemical impedance spectroscopy. Polarization results revealed that Metformin acted as mixed type inhibitors. The inhibition efficiency increases with increasing the inhibitors concentration and decreases with increasing the temperature. The gravimetric and potentiodynamic polarization results were in good agreement with the electrochemical impedance spectroscopy data.

Keywords: A- Kinetic parameters; A-Mild steel;; B-EIS; C-Acid corrosion; C- Quantum calculations

1. INTRODUCTION

The corrosion behaviour of mild steel in acid solution is a subject of practical significance considering its widespread applications in industries. Acid solutions are commonly used in the removal of rust and scale developed in industrial process.

Specific interaction between molecular structure of inhibitor and metal surface is extensively studied [1]. Compounds that contain π -bonds generally exhibit good inhibitive properties by supplying electrons via the heteroatoms (N, S or O). When both these features combine, enhanced inhibition can be observed. Because of their natural origin [2], as well as their nontoxic characteristics [3] and negligible negative impacts on the environment, drugs (chemical medicines) seem to be ideal chemical molecules to replace traditional toxic corrosion inhibitors.

The following drugs were used as good inhibitors for mild steel corrosion in acidic solutions: Ceftriaxone, Cefalexin, Doxycycline, Pheniramine, Fexofenadine, Cefotaxime, Cefuroxime, Cefapirin, Dapsone, Mebendazole, Penicillin G, Penicillin V, Cefadroxil, Ampicillin, Sparfloxacin, Chloramphenicol, Ketoconazole, Methocarbamol, Orphenadrine, Cefotaxime and Cefazolin [4-24].

In this work, we purchased and studied Cetapin XR 500 mg marketed in India by Aventis Pharma Limited which contained Metformin hydrochloride as an active constituent with the IUPAC name *N,N*-dimethylimidodicarbonimidic diamide. Metformin has the structure (Fig. 1), molecular formula $C_4H_{11}N_5$ and Molecular mass 129.62 g/mol. The LD50 dose for Metformin is 200 mg/kg for Guinea Pig and the route is intramuscular [25]. The gravimetric and electrochemical techniques such as potentiodynamic polarization, impedance measurements and the geometry of the inhibitor in its ground state were also studied. Several isotherms were tested for their relevance to describe the adsorption behaviour of the compounds studied. The effect of temperature on the corrosion behaviour of steel in the absence and presence of inhibitors was also studied.

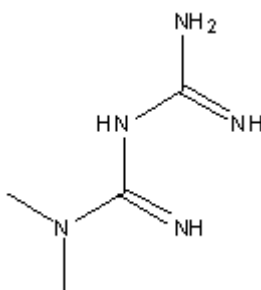


Figure 1. Structure of Metformin

2. EXPERIMENTAL

2.1 Inhibitor

Stock solutions of Metformin were made by dissolving it in 1 M hydrochloric acid to ensure solubility. This stock solution was used for all experimental purposes. The test solution of hydrochloric acid (AR grade) is used for all studies. Double distilled water is used for dilution.

2.2 Corrosion measurements

Prior to all measurements, the mild steel specimens, having composition (wt %) Fe 99.30%, C 0.076%, Si 0.026%, Mn 0.192%, P 0.012%, Cr 0.050%, Ni 0.050%, Al 0.023%, and Cu 0.135%, were abraded successively with emery papers from 600 to 1200 mesh/in grade. The specimen were washed thoroughly with double distilled water, degreased with acetone and finally dried in hot air blower. After drying, the specimen were placed in desiccator and then used for experiment. The aggressive solution of 1 M HCl was prepared by dilution of analytical grade HCl (37%) with double distilled water and all experiments were carried out in unstirred solutions. The rectangular specimens with

dimension $2.5 \times 2.0 \times 0.025 \text{ cm}^3$ were used in weight loss experiments and of size $1.0 \times 1.0 \text{ cm}^2$ (exposed) with a 7.5 cm long stem (isolated with commercially available lacquer) were used for electrochemical measurements.

2.3. Weight loss method

Weight loss measurements were performed on rectangular mild steel samples having size $2.5 \times 2.0 \times 0.025 \text{ cm}^3$ by immersing the mild steel coupons into acid solution (100 mL) in absence and presence of different concentrations of Metformin. After the elapsed time, the specimen were taken out, washed, dried and weighed accurately. All the tests were conducted in aerated 1 M HCl. All the experiments were performed in triplicate and average values were reported. The inhibition efficiency (η %) and surface coverage (θ) were determined by using following equation;

$$\theta = \frac{w_o - w_i}{w_o} \quad (1)$$

$$\eta\% = \frac{w_o - w_i}{w_o} \times 100 \quad (2)$$

where w_i and w_o are the weight loss values in presence and absence of inhibitor, respectively.

The corrosion rate (C_R) of mild steel was calculated using the relation:

$$C_R (\text{mmy}^{-1}) = \frac{87.6 \times w}{AtD} \quad (3)$$

where w is weight loss of mild steel (mg), A the area of the coupon (cm^2), t is the exposure time (h) and D the density of mild steel (g cm^{-3}) [26].

2.4 Electrochemical impedance spectroscopy

The EIS tests were performed at 308 K in a three electrode assembly. A saturated calomel electrode was used as the reference; a 1 cm^2 platinum foil was used as counter electrode. All potentials are reported versus SCE. Electrochemical impedance spectroscopy measurements (EIS) were performed using a Gamry instrument Potentiostat/Galvanostat with a Gamry framework system based on ESA 400 in a frequency range of 10^{-2} Hz to 10^5 Hz under potentiodynamic conditions, with amplitude of 10 mV peak-to-peak, using AC signal at E_{corr} . Gamry applications include software DC105 for corrosion and EIS300 for EIS measurements, and Echem Analyst version 5.50 software packages for data fitting. The experiments were carried out after 30 min. of immersion in the testing solution (no deaeration, no stirring).

The inhibition efficiency of the inhibitor was calculated from the charge transfer resistance values using the following equation:

$$\mu\% = \frac{R_{ct}^i - R_{ct}^0}{R_{ct}^i} \times 100 \quad (4)$$

where, R_{ct}^0 and R_{ct}^i are the charge transfer resistance in absence and in presence of inhibitor, respectively.

2.5 Potentiodynamic polarization

The electrochemical behaviour of mild steel sample in inhibited and uninhibited solution was studied by recording anodic and cathodic potentiodynamic polarization curves. Measurements were performed in the 1 M HCl solution containing different concentrations of the tested inhibitor by changing the electrode potential automatically from -250 to +250 mV versus corrosion potential at a scan rate of 1 mV s⁻¹. The linear Tafel segments of anodic and cathodic curves were extrapolated to corrosion potential to obtain corrosion current densities (i_{corr}). From the polarization curves obtained, the corrosion current (i_{corr}) was calculated by curve fitting using the equation:

$$I = i_{corr} \left[\exp\left(\frac{2.3\Delta E}{b_a}\right) - \exp\left(-\frac{2.3\Delta E}{b_c}\right) \right] \quad (5)$$

The inhibition efficiency was evaluated from the measured i_{corr} values using the relationship:

$$\mu\% = \frac{i_{corr}^0 - i_{corr}^i}{i_{corr}^0} \times 100 \quad (6)$$

where, i_{corr}^0 and i_{corr}^i are the corrosion current density in absence and presence of inhibitor, respectively.

2.6 Linear polarization measurement

The corrosion behaviour was studied with polarization resistance measurements (R_p) in 1 M HCl solution with and without different concentrations of studied inhibitor. The linear polarization study was carried out from cathodic potential of -20 mV versus OCP to an anodic potential of +20 mV versus OCP at a scan rate 0.125 mV s⁻¹ to study the polarization resistance (R_p) and the polarization resistance was evaluated from the slope of curve in the vicinity of corrosion potential. From the evaluated polarization resistance value, the inhibition efficiency was calculated using the relationship:

$$\mu\% = \frac{R_p^i - R_p^0}{R_p^i} \times 100 \tag{7}$$

where, R_p^0 and R_p^i are the polarization resistance in absence and presence of inhibitor, respectively.

3. RESULTS AND DISCUSSION

3.1 Electrochemical impedance spectroscopy

Impedance method provides information about the kinetics of the electrode processes and simultaneously about the surface properties of the investigated systems. The shape of impedance gives mechanistic information. Nyquist plots of mild steel in uninhibited and inhibited acid solution containing various concentrations of Metformin are presented in Fig. 2a. It followed from Fig. 2a that the impedance of the inhibited mild steel increases with increase in the inhibitor concentration and consequently the inhibition efficiency increased. A depressed semicircle is mostly referred to as frequency dispersion which could be attributed to different physical phenomena such as roughness and inhomogeneities of the solid surfaces, impurities, grain boundaries and distribution of the surface active sites [27].

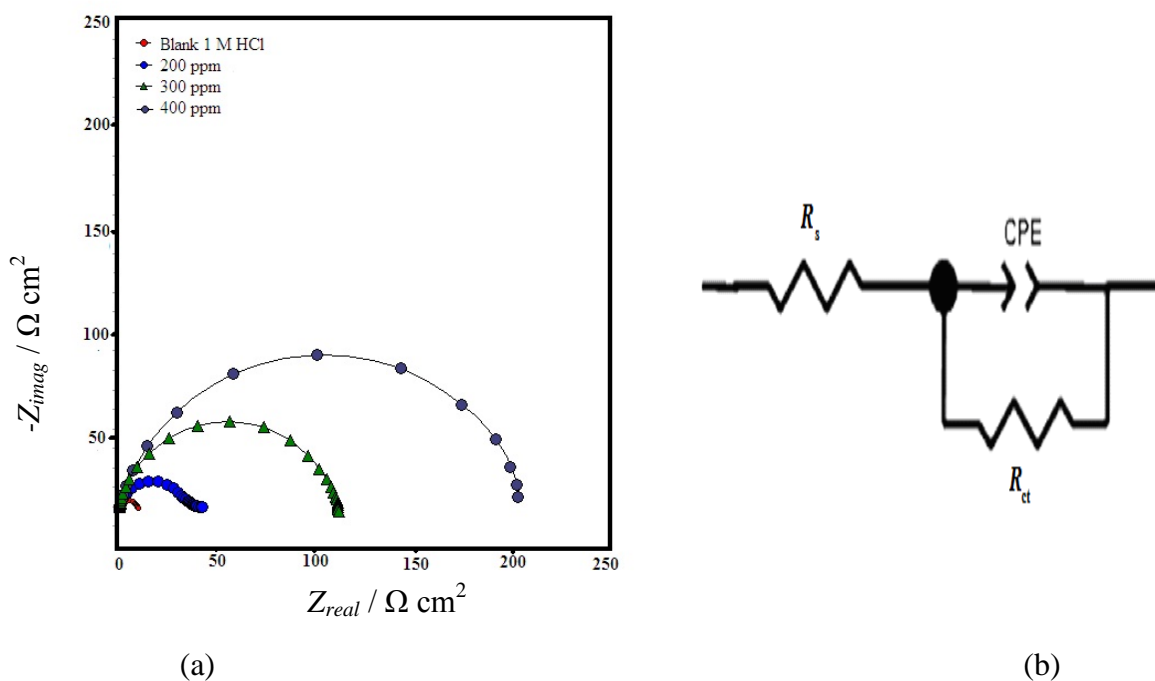


Figure 2. (a) Nyquist plots of mild steel in 1 M HCl in absence and presence of different concentrations of Metformin (b) equivalent circuit used to fit the impedance data

Different corrosion parameters derived from EIS measurements are presented as Table 1. It is shown from Table 1 that R_{ct} of inhibited system increased from $67 \Omega\text{cm}^2$ to $220 \Omega\text{cm}^2$ and double layer capacitance C_{dl} decreased from $43 \mu\text{Fcm}^{-2}$ to $23 \mu\text{Fcm}^{-2}$ with increasing inhibitor concentration. This decrease in C_{dl} results from a decrease in local dielectric constant and/or an increase in the thickness of the double layer, suggested that inhibitor molecules inhibit the iron corrosion by adsorption at the metal/acid interface.

To get more accurate fit of these experimental data, the measured impedance data were analyzed by fitting in to equivalent circuit given in Fig. 2b. Excellent fit with this model was obtained for all experimental data.

Mathematically, amplitude of CPE is given by the relation:

$$Z_{CPE} = Q^{-1}(j\omega)^{-n} \tag{8}$$

where Q is the magnitude of the CPE, j is the imaginary unit, ω is the angular frequency ($\omega = 2\pi f$, the frequency in Hz), and n is the phase shift which gives details about the degree of surface inhomogeneity. When $n = 1$, this is the same equation as that for the impedance of a capacitor, where $Q = C_{dl}$. In fact, when n is close to 1, the CPE resembles a capacitor, but the phase angle is not 90° . It is constant and somewhat less than 90° at all frequencies.

The electrochemical parameters, Including are listed in Table 1. C_{dl} values derived from CPE parameters are listed in Table 1. For providing simple comparison between the capacitive behaviors of different corrosion systems, the values of Q were converted to C_{dl} using the relation [28]:

$$C_{dl} = Q(\omega_{max})^{n-1} \tag{9}$$

here, ω_{max} represents the frequency at which the imaginary component reaches a maximum. It is the frequency at which the real part (Z_r) is midway between the low and high frequency x-axis intercepts.

Table 1. Calculated electrochemical parameters for mild steel in absence and presence of different concentrations of Metformin

Inhibitor	Conc. (ppm)	Tafel data					Linear polarization data			EIS data				
		-Ecorr (mv vs. SCE)	icorr ($\mu\text{A cm}^{-2}$)	β_a (mV d-1)	β_c (mV d-1)	$\mu\%$	Rp ($\Omega\text{ cm}^2$)	$\mu\%$	Rs ($\Omega\text{ cm}^2$)	Q ($\Omega^{-1}\text{sn cm}^{-2}$)	n	Rct ($\Omega\text{ cm}^2$)	Cdl ($\mu\text{F cm}^{-2}$)	$\mu\%$
	Blank	446	1540	90	121	-	8	-	1.20	250	0.827	8	69	-
Metformin	200	480	194	67	96	87	49	84	1.02	67	0.840	67	43	88
	300	441	163	73	146	89	77	90	1.05	48	0.850	116	31	93
	400	462	112	94	167	93	129	94	1.84	95	0.865	220	23	96

3.2 Potentiodynamic Polarization

The Tafel polarization curves of mild steel in hydrochloric acid solution, in the absence and presence of different concentrations of Metformin, are presented in Fig. 3 and listed in Table 1. The maximum inhibition efficiency (94%) was obtained at a concentration of 400 ppm.

Addition of the Metformin to acid media affected both the cathodic and anodic parts of the curves. For the inhibited system, if the displacement in E_{corr} value is greater than 85 mV relative to uninhibited system than the inhibitor is classified as cathodic or anodic type. In our case, the maximum displacement of E_{corr} value is 39 mV, hence the Metformin is classified as a mixed-type inhibitor. From the polarization curves it was noted that the curves were shifted toward lower current density region and β_c and β_a values increased with increase of concentration of inhibitor compounds. The higher β_c and β_a values indicated the retardation of both anodic and cathodic reactions. The inhibition efficiency values in the Table 1 showed that the Metformin acted as very effective corrosion inhibitor for mild steel in HCl solution and its capacity of inhibition increased with increase of concentration.

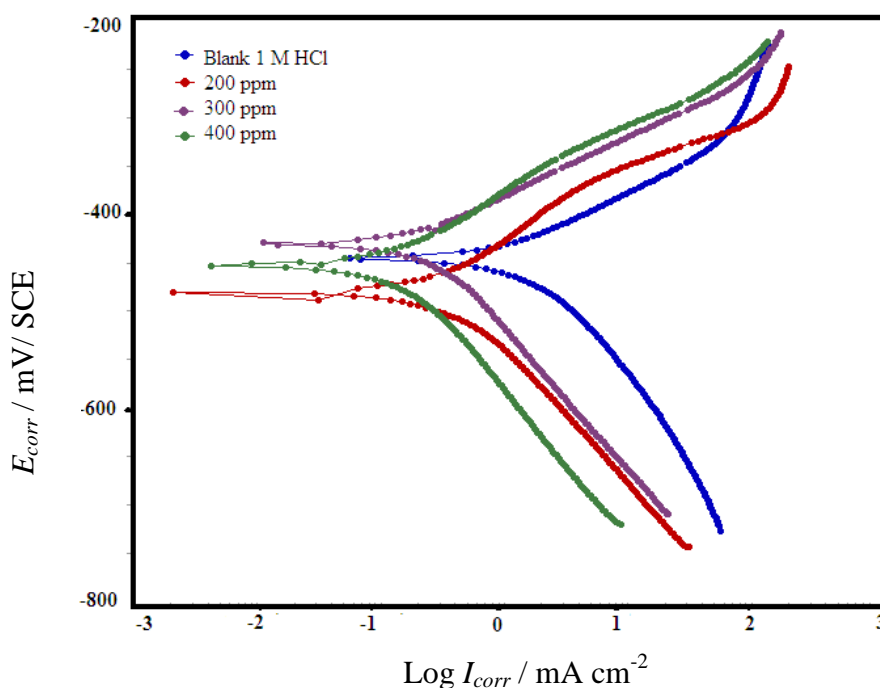


Figure 3. Tafel polarization curves for corrosion of mild steel in 1 M HCl in the absence and presence of different concentrations of Metformin

3.3 Linear polarization measurement

The inhibition efficiencies and polarization resistance parameters are presented in Table 1. The results obtained from Tafel polarization and EIS showed good agreement with the results obtained from linear polarization resistance.

3.4 Weight loss measurements

3.4.1 Effect of inhibitor concentration

The effect of inhibitor concentration on inhibition efficiency of steel in 1 M HCl was examined. Maximum inhibition efficiency of 95% was shown at 400 ppm in HCl solution. The values of percentage inhibition efficiency ($\eta\%$) and corrosion rate (C_R) obtained from weight loss method at different concentrations of Metformin at 308 K are summarized in Table 2.

Table 2. Corrosion rate and Inhibition efficiency values for the corrosion of mild steel in aqueous solution of 1 M HCl in the absence and in the presence of different concentrations of Metformin from weight loss measurements at 308 K

Name of Inhibitor	Conc. of Inhibitor (ppm)	Surface Coverage (θ)	$\eta\%$	CR (mmy-1)
-	-	-	-	77
Metformin	100	0.59	59	32
	200	0.72	72	21
	300	0.87	87	10
	400	0.95	95	4

3.4.2 Effect of temperature

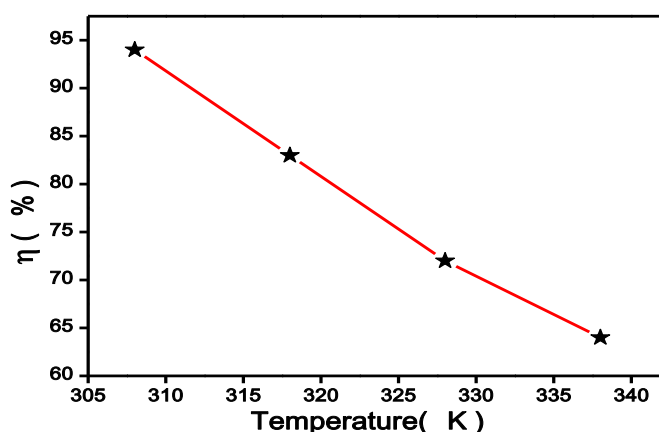


Figure 4. Inhibition efficiency of Metformin at different temperatures

In order to investigate the effect of temperature on the performance of studied inhibitor and to derive thermodynamic activation and adsorption parameters, weight loss studies were performed at

four different temperatures as depicted in Figure 4. The inhibition efficiency of Metformin decreases with increasing temperature.

3.4.3 Thermodynamic activation parameters

The dependence of corrosion rate at temperature can be expressed by Arrhenius equation and transition state equation:

$$\log(C_R) = \frac{-E_a}{2.303RT} + \log \lambda \tag{10}$$

$$C_R = \frac{RT}{Nh} \exp\left(\frac{\Delta S^*}{R}\right) \exp\left(-\frac{\Delta H^*}{RT}\right) \tag{11}$$

where E_a apparent activation energy, λ the pre-exponential factor, ΔH^* the apparent enthalpy of activation, ΔS^* the apparent entropy of activation, h Planck's constant and N the Avogadro number.

The apparent activation energy for Metformin is presented in Table 3. As it can be seen from Table 3, the values of activation free energy of Metformin are higher than that of free acid solution. Thus, the corrosion rate of mild steel is mainly controlled by activation parameters.

The linear regression between $\log(C_R)$ vs. $1/T$ and $\log(C_R/T)$ vs. $1/T$ were performed. Straight lines obtained with a slope $(-\Delta E_a/2.303R)$, $(-\Delta H^*/2.303R)$ and an intercept of $[\log(R/Nh) + (\Delta S^*/2.303R)]$, from which the value of E_a , ΔH^* and ΔS^* were calculated and presented in Table 3.

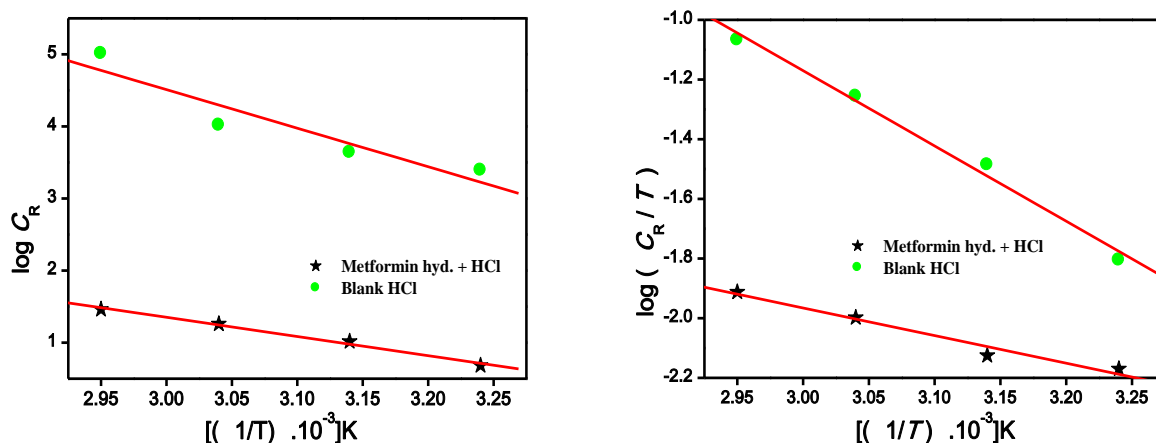
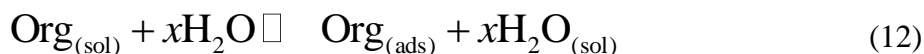


Figure 5. (a) Arrhenius plots of log CR versus 1/T (b) Transition state plots of log CR/T versus 1/T

3.4.4 Thermodynamic parameters and adsorption isotherm

The efficiency of Metformin molecules as a successful corrosion inhibitor mainly depends on their adsorption ability on the metal surface. To emphasize the nature of adsorption, the adsorption of an organic adsorbate at metal/solution interface can be presented as a substitution adsorption process between the organic molecules in aqueous solution $Org_{(sol)}$, and the water molecules on metallic surface $H_2O_{(ads)}$:



where, x is the size ratio representing the number of water molecules replaced by one molecule of organic adsorbate, $Org_{(sol)}$ and $Org_{(ads)}$ are the organic molecules in the solution and adsorbed on the metal surface, respectively. It is essential to know the mode of adsorption and the adsorption isotherm that can give important information on the interaction of inhibitor and metal surface. Attempts were made to fit surface coverage values determined from weight loss measurements into different adsorption isotherm models (Figure 6a-c). The linear regression coefficient values (R^2) determined from the plotted curves were found to be in the range of 0.99641 for Langmuir, 0.98179 for Temkin and 0.95116 for Frumkin adsorption isotherms at different temperatures studied. According to these results, it can be concluded that the best description of the adsorption behaviour of Metformin can be best explained by Langmuir adsorption isotherm given by equation (13).

Langmuir adsorption isotherm can be expressed by following equation:

$$\frac{C_{(inh)}}{\theta} = \frac{1}{K_{(ads)}} + C_{(inh)} \tag{13}$$

where, C_{inh} is inhibitor concentration and K_{ads} is an equilibrium constant for adsorption-desorption process.

Table 3. Thermodynamic parameters for the adsorption of Metformin in 1 M HCl on the mild steel

Inhibitor	Conc. (ppm)	E_a (kJ mol ⁻¹)	$-\Delta G_{ads}^{\circ}$ (kJ mol ⁻¹)	ΔH_{ads}° (kJ mol ⁻¹)	ΔS_{ads}° (J K ⁻¹ mol ⁻¹)
Blank	0	28.77	-	22.17	-136.90
Metformin	400	51.52	32	48.84	-73

The standard free energy of adsorption of inhibitor (ΔG_{ads}°) on mild steel surface can be evaluated with the following equation:

$$\Delta G_{\text{ads}}^{\circ} = -RT \ln(55.5 K_{\text{ads}}) \quad (14)$$

The negative values of standard free energy of adsorption indicated spontaneous adsorption of Metformin on mild steel surface and also strong interaction and stability of the adsorbed layer with the steel surface [29, 30].

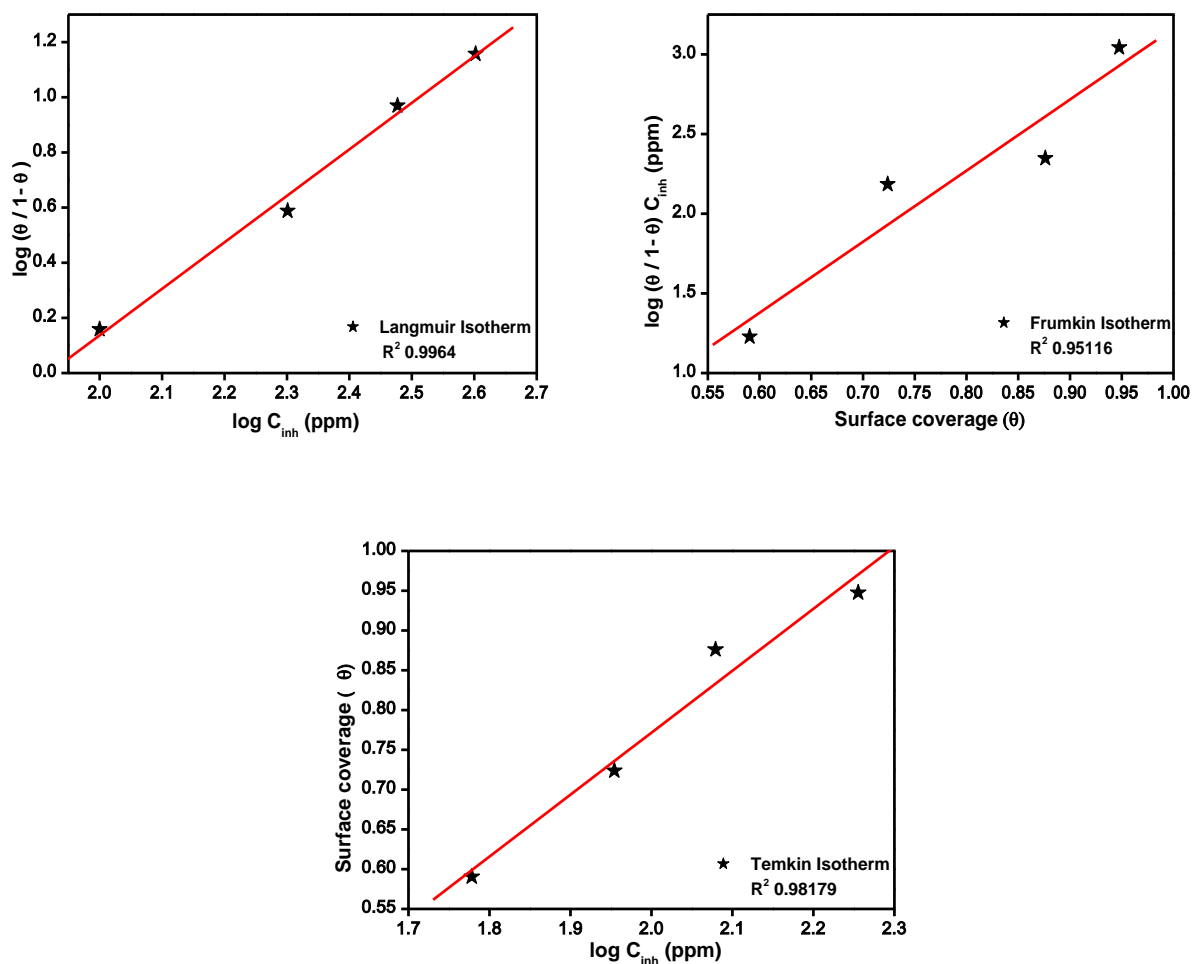


Figure 6. (a) Langmuir (b) Frumkin and (c) Temkin adsorption isotherm plots for the adsorption of Metformin on the surface of mild steel,

3.5. Quantum Chemical Calculations

Quantum chemical calculations were carried out in order to investigate adsorption and inhibition mechanism of studied inhibitor molecules. Fig. 7 show full geometry optimization of the inhibitor molecules with Mulliken charges. The Frontier molecular orbital (FMO) density distributions of Metformin are presented in Fig. 8 (a-b). In order to construct a composite index of an inhibitor molecule it may be important to focus on parameters that directly influence the electronic interaction

of the inhibitor molecules with the metal surface. These are mainly: E_{HOMO} , E_{LUMO} , ΔE ($E_{\text{LUMO}} - E_{\text{HOMO}}$), and dipole moment μ . The values of calculated quantum chemical parameters such as E_{HOMO} , E_{LUMO} , ΔE ($E_{\text{LUMO}} - E_{\text{HOMO}}$), and μ of Metformin are listed in Table 4.

As E_{HOMO} is often associated with the electron donating ability of a molecule, high values of E_{HOMO} are likely to indicate a tendency of the molecule to donate electrons to appropriate acceptor molecules with low-energy, empty molecular orbital. Increasing values of the E_{HOMO} facilitate adsorption (and therefore inhibition) by influencing the transport process through the adsorbed layer. Therefore, the energy of the E_{LUMO} indicates the ability of the molecule to accept electrons; hence these are the acceptor states. The lower the value of E_{LUMO} , the more probable, it is that the molecule would accept electrons [31]. As for the values of ΔE ($E_{\text{LUMO}} - E_{\text{HOMO}}$) concern; lower values of the energy difference ΔE will cause higher inhibition efficiency because the energy to remove an electron from the last occupied orbital will be low [32]. For the dipole moment (μ), lower values of μ will favor accumulation of the inhibitor in the surface layer.

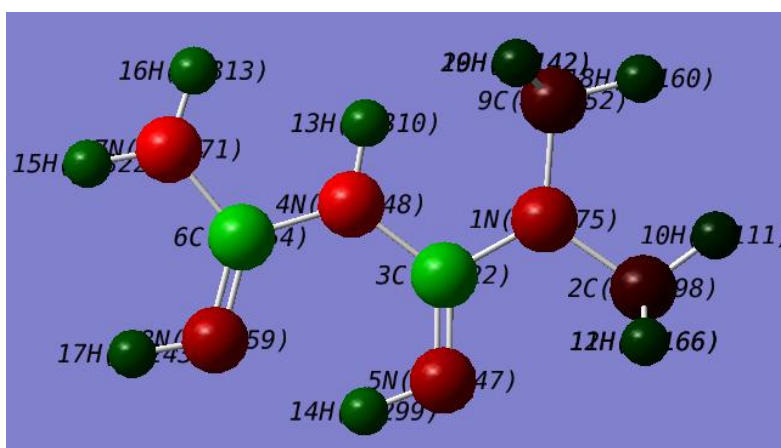


Figure 7. Optimized molecular structure with Mulliken charges of Metformin

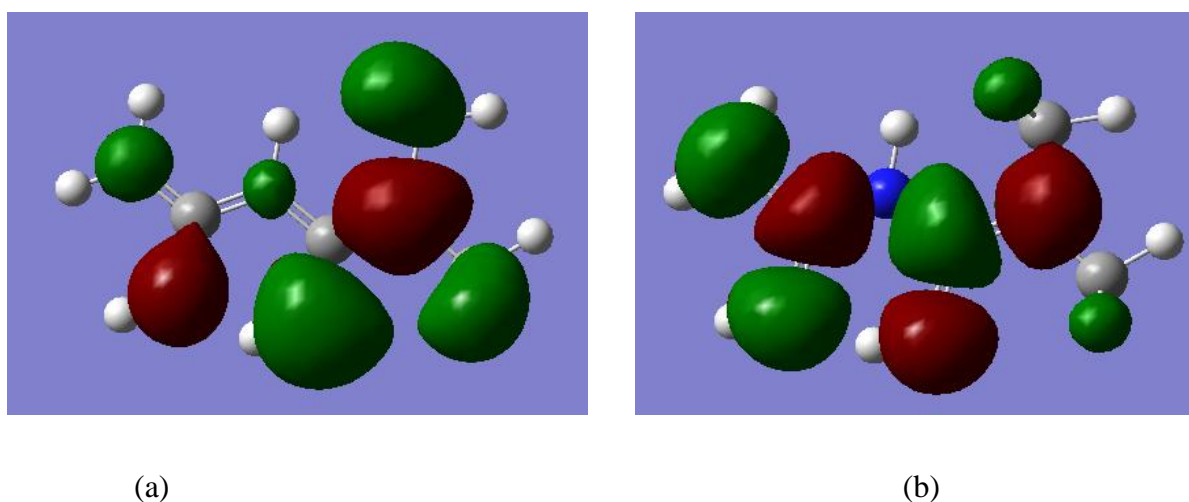


Figure 8. The frontier molecular orbital density distribution of Metformin (a) HOMO (b) LUMO

Table 4. Calculated Quantum chemical parameters of studied inhibitors

Quantum Parameters	Metformin
HOMO (hartree)	-0.19043
LUMO (hartree)	0.04090
ΔE LUMO-HOMO (hartree)	0.23133
Dipole Moment (μ)	3.2432

4. MECHANISM OF INHIBITION

Adsorption of Metformin arises from the donor acceptor interactions between free electron pairs of hetero atoms and π -electrons of multiple bonds, vacant d-orbitals of S-atom and vacant d-orbitals of Fe. In case of adsorption of organic compounds on the metallic surface, planarity of molecules must also be taken in to consideration. The protonated Metformin may adsorb on surface through synergistic effect with Cl^- in hydrochloric acid solution [33]. It is well known fact that the inhibitors which not only offer d electrons but also have unoccupied orbitals, so exhibit a tendency to accept electrons from d-orbital of metal to form stable chelates which are considered as excellent inhibitor [34].

The adsorption of organic molecules on the solid surfaces cannot be considered only as purely physical or as purely chemical adsorption phenomenon. In addition to the chemical adsorption, inhibitor molecules can also be adsorbed on the steel surface via electrostatic interaction between the charged metal surface and charged inhibitor molecule if it is possible [35, 36].

5. CONCLUSIONS

1. The inhibitor studied has an excellent inhibition effect for the corrosion of mild steel in 1 M HCl. The high inhibition efficiencies of were attributed to the adherent adsorption of the inhibitor molecules on the mild steel surface.
2. The adsorption of these compounds on the mild steel surface obeyed the Langmuir adsorption isotherm.
3. Potentiodynamic polarization studies revealed that the studied inhibitor is mixed type inhibitor.
4. The results demonstrate that the inhibition by the Metformin were attributable to the adsorption of molecules on mild steel surface. On the other hand, values of the obtained double layer capacitance (C_{dl}) have shown a tendency to decrease, which can result from a decrease in local dielectric constant and/or an increase in thickness of the electrical double layer.

5. Quantum chemical approach is adequately sufficient to predict the structure and molecule suitability to be an inhibitor.

References

1. M. Lagrene, B. Mernari, M. Bouanis, M. Traisnel and F. Bentiss, *Corros. Sci.* 44 (2002) 573.
2. Z. Tao, S. Zhang, W. Li and B. Hou, *Corros. Sci.* 51 (2009) 2588.
3. S. Struck, U. Schmidt, B. Gruening, I.S. Jaeger, J. Hossbach and R. Preissner, *Genome Inform.* 20 (2008) 231.
4. M.A. Quraishi and S. K. Shukla. *Journal of Appl. Electrochem.* 39 (2009), 1517.
5. S. K. Shukla and M. A. Quraishi, *Mater. Chem. Phys.* 120 (2010) 142.
6. S. K. Shukla and M. A. Quraishi, *Corros. Sci.* 52 (2010) 314.
7. I. Ahamad, R. Prasad and M. A. Quraishi, *Corros. Sci.* 52 (2010) 3033.
8. I. Ahamad, R. Prasad and M. A. Quraishi, *Journal of Solid State Electrochem.* 14 (2010) 2095.
9. A. K. Singh and M. A. Quraishi. *Journal of Applied Electrochem.* 41 (2011) 7.
10. A.K. Singh, M. A. Quraishi and Eno E. Ebenso, *Int. J. Electrochem. Sci.*, 6 (2011) 5676.
11. A.K. Singh, Eno E. Ebenso and M. A. Quraishi, *Int. J. Electrochem. Sci.* 7 (2012) 2320.
12. Ambrish Singh, A. K. Singh and M. A. Quraishi, *The Open Electrochem. J.* 2 (2010) 43.
13. I. Ahamad and M. A. Quraishi, *Corros. Sci.* 52, (2010), 651.
14. N. O. Eddy, S. A. Odoemelam and P. Ekwumemgbo, *Sci. Res. Essays* 4 (2009) 33.
15. N. O. Eddy and S. A. Odoemelam, *Adv. Nat. Appl. Sci.* 2 (2008) 225.
16. S. K. Shukla, M. A. Quraishi and Eno E. Ebenso, *Int. J. Electrochem. Sci.* 6 (2011) 2912.
17. N. O. Eddy, Eno E. Ebenso and U. J. Ibok, *J. Appl. Electrochem.* 40 (2010) 445.
18. S. K. Shukla, Eno E. Ebenso and M. A. Quraishi, *Int. J. Electrochem. Sci.* 6 (2011) 2912.
19. N. O. Eddy, S. R. Stoyanov, Eno E. Ebenso, *Int. J. Electrochem. Sci.* 5 (2010) 1127.
20. N. O. Eddy, U. J. Ibok, Eno E. Ebenso, A. El Nemr and E.S.H. El Ashry, *J. Mol. Mod.* 15 (2009) 1085.
21. I. B. Obot, *Port. Electrochim. Acta.* 27 (2009) 539.
22. Eno E. Ebenso, N. O. Eddy and A. O. Odiongenyi, *Port. Electrochim. Acta.* 27 (2009) 13.
23. S. K. Shukla and M. A. Quraishi, *Corros. Sci.* 51(2009) 1007.
24. A. K. Singh and M. A. Quraishi, *Corros. Sci.* 52 (2010) 152.
25. B. Melander, *Toxicol. Appl. Pharmacol.* 2 (1960) 47.
26. Mars G. Fontana, *Corrosion Engineering*, Mcgrawhill, Singapore, (1987) 173.
27. K. Juttner, *Electrochim. Acta.* 35 (1990) 1501.
28. C. S. Hsu and F. Mansfeld, *Corrosion.* 57 (2001) 747.
29. A. K. Singh and M. A. Quraishi, *Corros. Sci.* 52 (2010) 152.
30. F. Zucchi, G. Trabaneli and G. Brunoro, *Corros. Sci.* 33 (1992) 1135.
31. G. Gece, *Corros. Sci.* 50 (2008) 2981.
32. R. M. Issa, M. K. Awad and F. M. Atlam, *Appl. Surf. Sci.* 255 (2008) 2433.
33. M. A. Quraishi and J. Rawat, *Mater. Chem. Phys.* 73 (2002) 118.
34. S. L. Li, Y. G. Wang, S. H. Chen, R. Yu, S. B. Lei, H.Y. Ma and D.X. Lin, *Corros. Sci.* 41(1999) 1769.
35. Ambrish Singh, I. Ahamad, D. K. Yadav, V. K. Singh and M. A. Quraishi, *Chem. Engg. Comm.* 199 (2012) 63.
36. Ambrish Singh, I Ahamad, V. K. Singh and M. A. Quraishi, *J. Solid State Electrochem.* 5 (2011) 1087.